Prediction of the Circumferential Film Thickness Distribution in Horizontal Annular Gas-Liquid Flow

E. T. Hurlburt and T. A. Newell

ACRC TR-111 February 1997

For additional information:

Air Conditioning and Refrigeration Center
University of Illinois
Mechanical & Industrial Engineering Dept.
1206 West Green Street
Urbana, IL 61801

(217) 333-3115

Prepared as part of ACRC Project 71
Two-Phase Modeling of Refrigerant and Refrigerant-Oil Mixtures Over Enhanced/Structured Surfaces
T. A. Newell, Principal Investigator

The Air Conditioning and Refrigeration Center was founded in 1988 with a grant from the estate of Richard W. Kritzer, the founder of Peerless of America Inc. A State of Illinois Technology Challenge Grant helped build the laboratory facilities. The ACRC receives continuing support from the Richard W. Kritzer Endowment and the National Science Foundation. The following organizations have also become sponsors of the Center.

Amana Refrigeration, Inc.
Brazeway, Inc.
Carrier Corporation
Caterpillar, Inc.
Copeland Corporation
Dayton Thermal Products
Delphi Harrison Thermal Systems
Eaton Corporation
Ford Motor Company
Frigidaire Company
General Electric Company
Hydro Aluminum Adrian, Inc.
Lennox International, Inc.
Modine Manufacturing Co.
Peerless of America, Inc.
Redwood Microsystems, Inc.
The Trane Company
Whirlpool Corporation

For additional information:

Air Conditioning & Refrigeration Center
Mechanical & Industrial Engineering Dept.
University of Illinois
1206 West Green Street
Urbana IL 61801

217 333 3115

Prediction of the Circumferential Film Thickness Distribution in Horizontal Annular Gas-Liquid Flow

Evan T. Hurlburt and Ty A. Newell

ABSTRACT

This paper develops a liquid film symmetry correlation and a liquid film thickness distribution model for horizontal annular gas-liquid pipe flows. The symmetry correlation builds on the work of Williams et al. (1996). A new correlating parameter is presented. The experimental data used in the correlation is from all three of the horizontal annular flow regions: stratified-annular, asymmetric annular, and symmetric annular. The liquid film thickness model is based on work done by Laurinat et al. (1985). The circumferential momentum equation is simplified to a balance between the normal Reynolds stress in the circumferential direction and the circumferential component of the weight of the film. A model for the normal Reynolds stress in the circumferential direction is proposed. The symmetry correlation is used to close the model equations. Circumferential film thickness distribution predictions are made in the three horizontal annular flow regions and compared to experimental data.

1. INTRODUCTION

The circumferential film thickness distribution in horizontal annular air-water flows has been measured over a range of tube diameters by several researchers (Dallman 1978; Fukano and Ousaka 1989; Laurinat 1982; Paras and Karabelas 1991; Williams 1990). From these studies we begin to see how the local time averaged film thickness is influenced by the flow conditions. Two general observations from these experiments are: 1) the film thickness is small relative to the tube radius - typical local film thickness values are between one tenth and one thousandth of the tube radius; 2) the film is asymmetric - it is thicker on the bottom of the tube than on the top. The focus of this paper is on the prediction of the circumferential symmetry and the prediction of the circumferential film thickness distribution. We will first show a method of correlating the film symmetry and then develop the circumferential film thickness model.

Symmetry has been examined by Williams et al. (1996). In this work the Froude number, $Fr = U_{sg}/(gD)^{0.5}$, was used to correlate the data, where U_{sg} is the gas superficial velocity, and D is the tube diameter. The Froude number dependence shows the effect of the gas phase velocity on symmetry. The least symmetric annular flows occur at low gas velocities. Here the flow is just entering the annular flow regime and behaves in part like a stratified flow. At very high gas velocities the film approaches a symmetric condition with very little decrease in film thickness from

bottom to top. At intermediate gas velocities the flow can be either asymmetric or symmetric depending on the liquid phase mass flow rate.

Correlating the symmetry is a valuable method for examining the experimental data. Insight is gained into the flow parameters that influence the film thickness distribution. It suggests a method by which the boundary between the stratified-annular and asymmetric annular flow regions can be predicted. As will be shown later in this paper, the correlation of the symmetry also provides additional information to use in closing the circumferential film thickness distribution model.

A film thickness model that considered both momentum and mass balances was developed by Laurinat et al. (1985). In this model the stresses internal to the liquid film and the momentum transfers from the gas phase to the liquid phase are the dominant factors affecting the distribution of the liquid film. Laurinat's model has been the starting point for subsequent modeling efforts (e.g. Fukano and Ousaka 1989). It includes momentum balances in the axial, radial, and circumferential directions and a mass balance which accounts for the circumferential redistribution of mass by atomization and deposition of droplets.

Laurinat "tuned" flow condition dependent constants in his model so that model predictions agreed with experimental data. This allowed for an evaluation of the relative significance of each of the terms in the momentum balance on the film thickness distribution. For the flow conditions considered he concluded that the normal stress gradient due to liquid phase velocity fluctuations in the circumferential direction is the dominant factor controlling the distribution. The interfacial shear acting on the liquid surface due to secondary flow in the gas core was found to be of significance near the top of the tube. Atomization and deposition resulted in some film redistribution, but the effects were relatively small.

Lin et al. (1985) took circumferential film thickness measurements and compared them to predictions from Laurinat's model. The experimental data was at low gas superficial velocities in the stratified-annular region of the annular flow regime. At these velocities they concluded that the interfacial shear due to secondary gas flows plays an important role in distributing the liquid film.

Fukano and Ousaka (1989) modified Laurinat's model to more directly include the effects of the waves on the liquid surface. This was done using a model for the normal stress in the liquid that is a function of the static pressure gradient in the gas with the static pressure gradient arising due to waves on the liquid surface. The result is a continual flow of liquid up the tube walls in regions with disturbance waves and a downward draining flow in the flatter regions before and after the waves. Experimental evidence of this mechanism has been observed by Sutharshan et al. (1995). Interfacial shear due to secondary flows was assumed to be negligible in Fukano and Ousaka's model.

2. THEORY

(A) Liquid Film Circumferential Symmetry

Laurinat (1982) took time averaged circumferential film thickness measurements in a horizontal 5.08 cm inner diameter tube over a range of different air and water mass flow rates in the annular flow regime. Measurements were taken in 45 degree increments around the tube. A graph of Laurinat's data at four different flow conditions is shown in figures 1 and 2. Measurements from both sides of the tube are included for angles from the bottom of 45, 90, and 135 degrees. These four curves cover the range of symmetry conditions seen in annular flow. At low air mass flow rates the distribution is highly asymmetric with the majority of the liquid flowing along the bottom of the tube. As the air mass flow rate increases (for a given water mass flow rate) symmetry increases. At very high air mass flow rates the film becomes nearly symmetric.

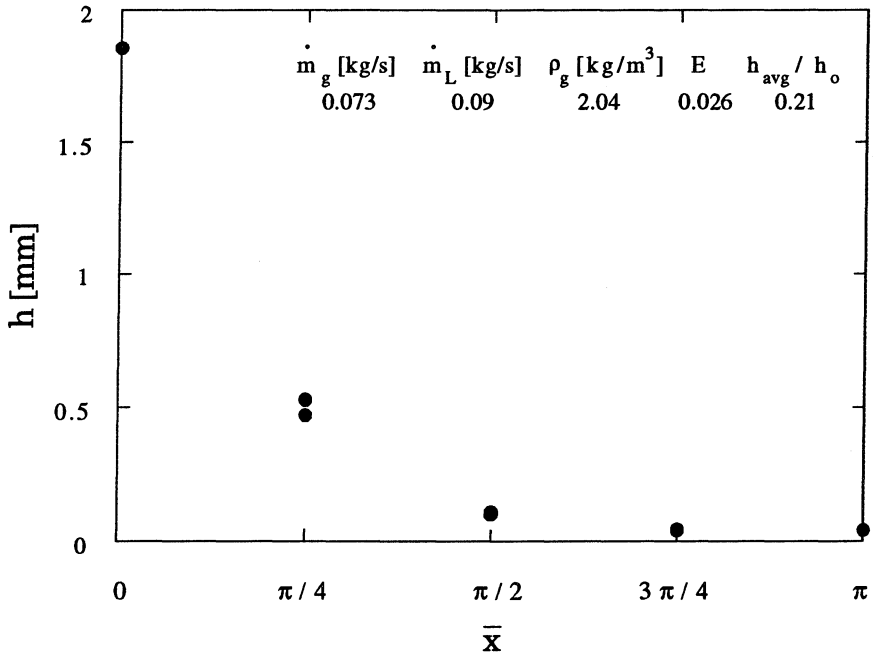

Figure 1 Film thickness measurements versus angle. Air- water data from Laurinat (1982) in a 5.08 cm diameter horizontal tube at an L/D of 300.

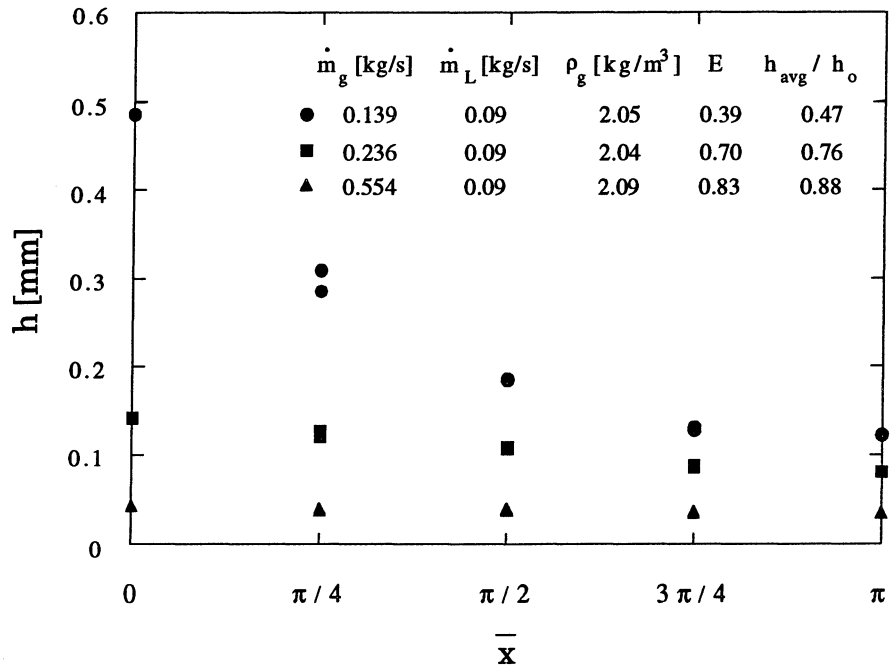

Figure 2 Film thickness measurements versus angle. Air-water data from Laurinat (1982) in a 5.08 cm diameter horizontal tube at an L/D of 300.

Various parameters have been used to quantify symmetry. Williams et al. (1996) used the integrated cross sectional area to define the symmetry parameter, $A_L / (h_o D)$. Here, A_L is the cross sectional area of the film, $A_L = \int_0^{\pi} (D - 2h)\, h\, d\theta$, h is the local film thickness, h_o is the film thickness at the bottom of the tube, D is the tube diameter, and θ is the angle from the tube bottom. As the flow becomes more symmetric, $A_L / (h_o D)$ approaches its maximum value, $\pi (1 - 2 m / D)$, where m is the average film thickness. It approaches its minimum value, $(4 / 3) (h_o / D)^{0.5}$, when the flow is stratified.

We will define the symmetry as the average film thickness divided by the film thickness at the bottom of the tube, h_{avg} / h_o, where h_{avg} is defined by the integral

$$h_{avg} = \frac{1}{\pi} \int_0^{\pi} h\, d\theta . \qquad [1]$$

This is a simplified form of Williams parameter with different limits. The parameter h_{avg} / h_o approaches its maximum value, 1, as the flow becomes more symmetric. It approaches its

minimum value, $(4 / (3\pi))\ (h_o / D)^{0.5}$, when the flow is stratified. The distributions in figures 1 and 2 are labeled with their h_{avg} / h_o values.

Williams correlated symmetry with the Froude number, $Fr = U_{sg}/(gD)^{0.5}$. Figure 3 shows this dependence, using the parameter h_{avg} / h_o, for measurements taken by Laurinat (1982) in a 5.08 cm diameter tube at an L/D of 300, where L is the distance from the point at which water enters the tube. Three different horizontal annular flow regions are apparent from this plot; stratified-annular at low U_{sg}, asymmetric annular at intermediate U_{sg}, and symmetric annular at high U_{sg}.

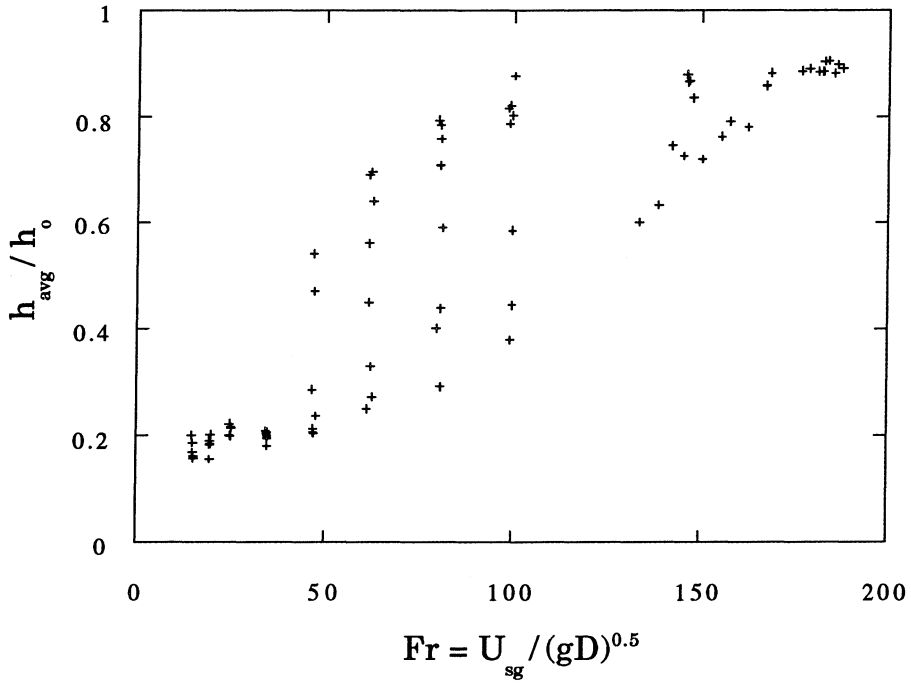

Figure 3 Symmetry parameter versus Froude. Air-water data from Laurinat (1982) in a 5.08 cm diameter horizontal tube at an L/D of 300.

The Froude number incorporates the effect of the gas mass flow rate on symmetry through the gas superficial velocity. It does not, however, account for the effect of the liquid mass flow rate. This is evident from the large scatter seen in the asymmetric annular flow region. In this region, as gas velocity increases for a given liquid mass flow rate the symmetry increases.

In order to include the liquid mass flow rate dependence and further collapse the data, other parameters besides the Froude number were investigated. The best correlation was found using the parameter $(\dot{m}_g / \dot{m}_L)^{0.5}$ Fr. This parameter is the square root of the ratio of the gas phase momentum flux, $\dot{m}_g U_{sg}$, to the power required to pump the liquid at it's mass flow rate from the

bottom of the tube to the top of the tube, $\dot{m}_L\, g\, D$. The mass flow rates used are the total gas mass flow rate and the total liquid mass flow rate.

A plot of h_{avg} / h_o vs. $(\dot{m}_g / \dot{m}_L)^{0.5}$ Fr using Laurinat's data is shown in figure 4. As seen from the plot, $(\dot{m}_g / \dot{m}_L)^{0.5}$ Fr eliminates most of the scatter that occurs when the symmetry parameter is plotted versus Fr.

Figure 4 is a plot of data taken at one tube diameter and one L/D. Figure 5 shows h_{avg} / h_o vs. $(\dot{m}_g / \dot{m}_L)^{0.5}$ Fr for a range of tube diameters and L/D's from a variety of different studies (Dallman 1978; Fukano and Ousaka 1989; Hurlburt and Newell 1996; Jayanti et al. 1990; Laurinat 1982; Paras and Karabelas 1991; Williams 1990). This larger data set has more scatter, but the general trend seen in figure 4 remains with the correlation significantly stronger than if h_{avg} / h_o were plotted versus Fr. The data sets showing a more rapid transition towards symmetric annular flow (Hurlburt and Newell (1996) and Jayanti et al. (1990)) are at the lowest L/D's. These flows may not be "fully developed" which is argued by Whalley (1987) to require an L/D of about 400.

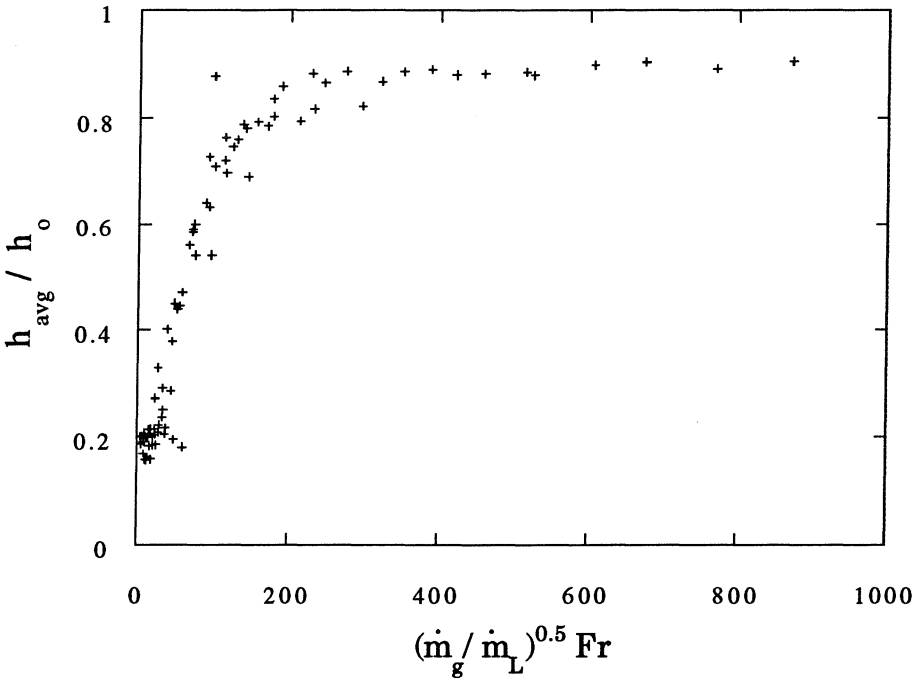

Figure 4 Symmetry parameter versus $(\dot{m}_g / \dot{m}_L)^{0.5}$ Fr. Air-water data from Laurinat (1982) in a 5.08 cm diameter horizontal tube at an L/D of 300.

The generality of h_{avg} / h_o vs. $(\dot{m}_g / \dot{m}_L)^{0.5}$ Fr at large L/D allows estimation of h_{avg} / h_o over a range of tube diameters. A curve fit to the data in figure 4 (valid for $(\dot{m}_g / \dot{m}_L)^{0.5}$ Fr > 20) is given by

$$\frac{h_{avg}}{h_o} = 0.2 + 0.7\left[1 - \exp\left(-\frac{(\dot{m}_g / \dot{m}_L)^{0.5}\,\mathrm{Fr} - 20}{75}\right)\right], \qquad [2]$$

where

$$\mathrm{Fr} = U_{sg}/(gD)^{0.5}\,. \qquad [3]$$

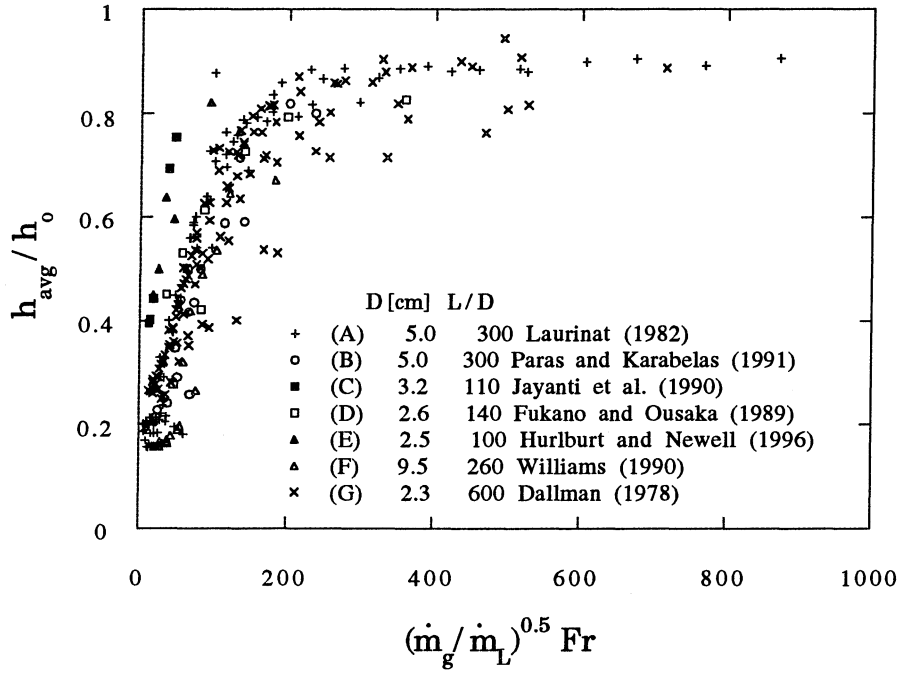

Figure 5 Symmetry parameter versus $(\dot{m}_g / \dot{m}_L)^{0.5}$ Fr. Air-water data from several separate studies at different diameters and different L/D's.

Figure 6 shows the data from figure 5 over the steeply rising part of the curve. Note the effect of diameter on the onset of the initial rise seen from Dallman (D = 2.3 cm), Laurinat (D = 5.08 cm), and Williams (D= 9.5 cm). This difference in the initial rise is not captured by [2] making the correlation least accurate in this region. A diameter dependence could be incorporated into the correlation by having the lower limit and the value subtracted from $(\dot{m}_g / \dot{m}_L)^{0.5}$ Fr in the exponential both functions of the tube diameter.

The correlation of h_{avg} / h_o with $(\dot{m}_g / \dot{m}_L)^{0.5}$ Fr allows for an estimation of the symmetry from knowledge of only the gas and liquid mass flow rates. A known value for h_{avg} / h_o is of

value in film thickness modeling. The added information on the average thickness of the distribution can be used to eliminate one of the constants in the model.

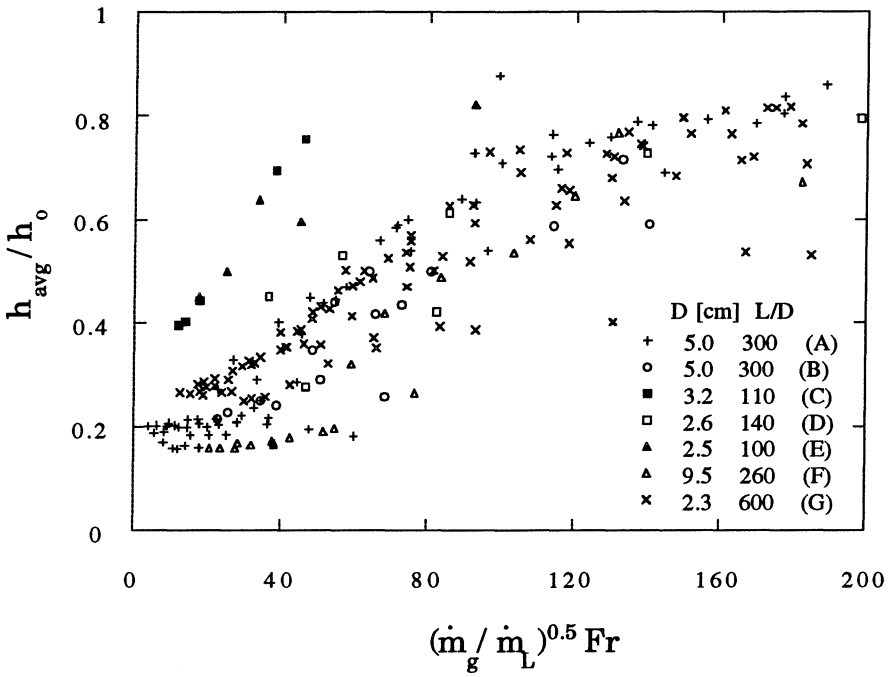

Figure 6 Data from figure 5 for $(\dot{m}_g / \dot{m}_L)^{0.5}$ Fr < 200.

(B) Prediction of the Circumferential Film Thickness Distribution

The momentum balance equations developed in Laurinat et al. (1985) are used to predict the film thickness. Some of the assumptions in this model include:

(1) The liquid film thickness is small relative to the tube radius. This allows for the use of Cartesian instead of cylindrical coordinates.

(2) The liquid phase is turbulent resulting in shear and normal stress forces due to gradients in the fluctuating velocities.

(3) The film height is not varying significantly with time. (The equations use time averaged quantities and predict the time averaged behavior.)

(4) The influence of waves on the liquid surface are accounted for indirectly through the interfacial axial shear model.

(5) The tube diameter is large enough that surface tension forces can be ignored.

(6) A constant pressure is imposed by the gas phase onto the surface of the liquid phase.

(7) τ_{xx} and τ_{xz} can be modeled as independent of radial position.

(8) The normal stress in the liquid scales with the liquid's axial velocity.

An implicit assumption is that gas entering the liquid, traveling through, and exiting the liquid as bubbles can be ignored. This process was observed by Hewitt et al. (1990).

The circumferential momentum balance is used to determine the film thickness. The radial momentum balance is used to eliminate the pressure gradient in the circumferential direction. The forces in the gas phase responsible for holding the liquid against the radial component of the film's weight are not considered.

Momentum Equations

The film thickness model uses Laurinat's development of the time-averaged momentum equations for fully-developed flow. The coordinate system is Cartesian with x as the circumferential direction, y as the radial direction, and z as the axial direction.

The axial momentum equation is

$$\frac{\partial \tau_{yz}}{\partial y} + \frac{1}{a}\frac{\partial \tau_{xz}}{\partial \bar{x}} = 0 \; . \qquad [4]$$

The circumferential momentum equation is

$$-\frac{1}{a}\frac{\partial p}{\partial \bar{x}} + \frac{\partial \tau_{yx}}{\partial y} + \frac{1}{a}\frac{\partial \tau_{xx}}{\partial \bar{x}} - \rho_L g \sin \bar{x} = 0 \; . \qquad [5]$$

The radial momentum equation is

$$-\frac{\partial p}{\partial y} - \rho_L g \cos \bar{x} = 0 \; . \qquad [6]$$

In these equations τ_{xx} and τ_{xz} are Reynolds stresses, τ_{yz} is the axial shear stress, τ_{yx} is the circumferential shear stress, p is the liquid pressure, ρ_L is the density of the liquid, and $\bar{x}$ is the circumferential distance from the bottom of the tube, x, divided by the tube radius, a.

Integration of [6] from any point, y, to the gas-liquid interface gives

$$-p|_h + p|_y - \rho_L g (h - y) \cos \bar{x} = 0 \; . \qquad [7]$$

Ignoring surface tension effects the interface pressure, $p|_h$, can be assumed equal to the gas phase pressure, p_o. If the gas phase pressure does not vary circumferentially, the radial momentum balance can be differentiated to solve for the static pressure gradient in the circumferential direction,

$$-\frac{1}{a}\frac{\partial p}{\partial \bar{x}} - \rho_L g \cos \bar{x} \frac{dh}{d\bar{x}} = 0 \; . \qquad [8]$$

Substitution of [8] into [5] gives

$$\frac{\partial \tau_{yx}}{\partial y} + \frac{1}{a}\frac{\partial \tau_{xx}}{\partial \bar{x}} - \rho_L g \sin \bar{x} - \rho_L g \cos \bar{x} \frac{dh}{d\bar{x}} = 0 \; . \qquad [9]$$

Equations [4] and [9] are non-dimensionalized using the shear for single-phase flow in a smooth tube,

$$\tau_s = 0.023\ Re_{sg}^{-0.2}\ \rho_g\ U_{sg}^2\ . \qquad [10]$$

Re_{sg} is the gas superficial Reynolds number and ρ_g is the density of the gas.

The resulting non-dimensional momentum balance equations describing the liquid film flow are

$$\frac{\partial \tau_{yz}^+}{\partial y^+} + \frac{1}{a^+}\frac{\partial \tau_{xz}^+}{\partial \bar{x}} = 0 \ , \qquad [11]$$

and

$$\frac{\partial \tau_{yx}^+}{\partial y^+} + \frac{1}{a^+}\frac{\partial \tau_{xx}^+}{\partial \bar{x}} - \frac{1}{a^+ Fr_{\tau_s}}\sin\bar{x} - \frac{1}{a^{+2} Fr_{\tau_s}}\cos\bar{x}\,\frac{dh^+}{d\bar{x}} = 0\ , \qquad [12]$$

where

$$Fr_{\tau_s} = \frac{\tau_s}{\rho_L g\, a}\ , \qquad [13]$$

and

$$h^+ = \frac{h}{\nu_L}\left(\frac{\tau_s}{\rho_L}\right)^{0.5} \qquad [14]$$

where ν_L is the kinematic viscosity of the liquid.

Simplification of the momentum equations

In this section further simplifications to the momentum equations will be made. The simplifications are based on the findings from Laurinat's evaluation of the relative impact of the terms in the momentum balance on the film thickness distribution. For the conditions considered these findings include:

(1) Atomization and deposition results in some film redistribution but the effects are relatively small.

(2) Interfacial circumferential shear due to secondary flows in the gas is significant only near the top of the tube.

(3) The static pressure gradient due to the circumferential film thickness gradient is small relative to the normal stress term.

(4) The dispersion term, $1/a^+\ (\partial \tau_{xz}^+ / \partial \bar{x})$, appears to be small relative to the axial shear.

The first simplification to the equations uses the result that the interfacial shear and atomization and deposition have only a small effect on the time averaged film distribution. When this is true, the local circumferential velocity, u, is zero (the time averaged upflow and downflow

are the same). The radial stress gradient, $\partial\tau^+_{yx}/\partial y^+$, can then be eliminated from [12] and the circumferential momentum balance becomes

$$\frac{\partial\tau^+_{xx}}{\partial\bar{x}} - \frac{1}{Fr_{\tau_s}}\sin\bar{x} - \frac{1}{a^+Fr_{\tau_s}}\cos\bar{x}\,\frac{dh^+}{d\bar{x}} = 0\ . \qquad [15]$$

The second simplification uses the finding that the static pressure gradient is small relative to the normal stress. This term is only of significance in the limit of fully stratified flows. Equation [15] then becomes

$$\frac{\partial\tau^+_{xx}}{\partial\bar{x}} - \frac{1}{Fr_{\tau_s}}\sin\bar{x} = 0\ . \qquad [16]$$

In this form, the circumferential component of the film's weight is balanced only by the circumferential normal stress gradient.

The final simplification to the momentum equations uses the result that the dispersion term, $1/a^+\,(\partial\tau^+_{xz}/\partial\bar{x})$, is small. The axial momentum balance [11] then becomes

$$\frac{\partial\tau^+_{yz}}{\partial y^+} = 0\ . \qquad [17]$$

This implies that the axial shear is constant in the radial direction. We will refer to this radially constant axial shear as the interfacial axial shear, τ^+_i, where $\tau^+_{yz} = \tau^+_{yz}\,|_h = \tau^+_i$.

τ^+_{xx} model

As is stated in the circumferential symmetry section, the film thickness distribution takes on three different characteristic shapes depending on the relative gas and liquid mass flow rates. These have been referred to in this paper as the stratified-annular, asymmetric annular, and symmetric annular regions of the horizontal annular flow regime. The characteristic shapes can be seen in figures 1 and 2. Stratified-annular flow shows a rapid decay in thickness from the bottom of the tube. Symmetric annular flow shows a very gradual decrease in film thickness from the bottom to the top of the tube. Asymmetric annular flow falls between these two extremes.

A model for τ^+_{xx} was developed that captures the behavior from these three regions. The normal Reynolds stress is considered to be a strong function of film thickness. For films of non-dimensional thickness less than 12, the Reynolds stress is assumed to increase linearly with film thickness, $\tau^+_{xx} = -C\,h^+$. For thicker films the Reynolds stress is assumed to increase less rapidly with film thickness, $\tau^+_{xx} = -C\ln(h^+)$. In order to avoid the use of two separate functions, a single exponential function that captures both the linear and logarithmic behavior will be used,

$$\tau^+_{xx} = -C_1\left(1 - \exp\left(-\frac{h^+}{12}\right)\right). \qquad [18]$$

The value of the parameter C_1 depends on the gas and liquid mass flow rates.

Circumferential film thickness solution

Using [18] for τ_{xx}^+, [16] becomes

$$-\frac{C_1}{12}\exp\left(-\frac{h^+}{12}\right)\frac{dh^+}{d\bar{x}}-\frac{1}{Fr_{\tau_s}}\sin\bar{x}=0\,. \qquad [19]$$

This differential equation can be solved analytically for h^+. The solution, which depends on the non-dimensional film thickness at the bottom of the tube, $h_o^+=(h_o/\nu_L)(\tau_s/\rho_L)^{0.5}$, is

$$\frac{h^+}{h_o^+}=\frac{\ln\left[\alpha-\beta(\cos\bar{x}-1)\right]}{\ln\alpha}\,, \qquad [20]$$

where

$$\alpha=\exp\left(-\frac{h_o^+}{12}\right), \qquad [21]$$

$$\beta=\frac{1}{C_1\,Fr_{\tau_s}}\,, \qquad [22]$$

and

$$Fr_{\tau_s}=\frac{\tau_s}{\rho_L\,g\,a}\,. \qquad [23]$$

Note that at large Fr_{τ_s}, h^+ approaches h_o^+ and the film approaches a symmetric condition.

Less complicated analytical solutions to [16] can be developed if the linear and the natural log models, $\tau_{xx}^+=-C\,h^+$ and $\tau_{xx}^+=-C\ln(h^+)$, are used. The disadvantage of this approach is that due to circumferential film thickness variation, each solution applies only over a range of angles. Equation [20], which uses the exponential model for τ_{xx}^+, [18], is a more complicated solution, but it applies at any angle.

The average film thickness can be found by integration of [20] from 0 to π. This results in a theoretical expression for the symmetry parameter,

$$\frac{h_{avg}^+}{h_o^+}=\frac{\ln\left[\dfrac{\alpha+\beta+\sqrt{\alpha^2+2\,\alpha\,\beta}}{2}\right]}{\ln\alpha}\,. \qquad [24]$$

Note that at large Fr_{τ_s}, h_{avg}^+ also approaches h_o^+.

When the total liquid and gas mass flow rates are known, the symmetry correlation [2] developed in section (2A) can be used to estimate the value of h_{avg}^+/h_o^+. With h_{avg}^+/h_o^+ known, C_1 becomes a function only of h_o^+.

To complete the film thickness distribution prediction, the film thickness at the bottom of the tube, h_o^+, must be determined. Prediction of h_o^+ requires an interfacial axial shear relation, a relation for the average axial velocity of the liquid film, mass conservation, and an entrainment

model which predicts the fraction of the total liquid mass flowing as droplets suspended in the gas core. Relations for the interfacial axial shear and the average axial velocity of the liquid film are developed in the following sections. An entrainment model is not developed in this paper. For comparison of model predictions to experimental data we assume the entrainment to be known.

τ_{yz} model

The term τ_{yz} is the local shear in the axial direction. From momentum balance considerations it is thought to be constant from the liquid-gas interface to the wall. As stated earlier, we will refer to this radially constant axial shear as the interfacial axial shear, τ_i^+, where $\tau_{yz}^+ = \tau_{yz}^+ |_h = \tau_i^+$

The interfacial axial shear has been determined experimentally via pressure drop and liquid film mass flow measurements by Asali and Hanratty (1985) for vertical air-water flows in the ripple regime ($Re_{LF} < 300$). The correlation found in this study shows interfacial axial shear to be a strong function of film thickness,

$$\frac{\tau_i}{\tau_s} - 1 = 0.45\, Re_g^{-0.2} \left(\phi\, h_i^+ - 4\right), \qquad [25]$$

where

$$\phi = \frac{\mu_L}{\mu_g}\left(\frac{\rho_g}{\rho_L}\right)^{0.5}, \qquad [26]$$

$$h_i^+ = \frac{h\, u_i^*}{\nu_L}, \qquad [27]$$

and

$$u_i^* = \sqrt{\frac{\tau_i}{\rho_L}}. \qquad [28]$$

Asali's interfacial shear correlation is based on vertical annular flow data. In this paper we assume the correlation to be applicable in predicting the local axial shear from the local film thickness in horizontal flows as well.

Asali's interfacial shear correlation is developed from data in which the product $\phi\, h_i^+$ is less than 100. In this region $\tau_i/\tau_s - 1$ shows the linear increase with non-dimensional film thickness seen in equation [25]. For films with $\phi\, h_i^+$ greater than 100 the rate of increase of $\tau_i/\tau_s - 1$ with film thickness is less rapid. An equation that captures this behavior over the entire film thickness range is

$$\frac{\tau_i}{\tau_s} - 1 = 10\left(1 - \exp\left(-\frac{\phi\, h_i^+}{250}\right)\right). \qquad [29]$$

Axial velocity

The liquid film average velocity can be estimated from the experimental correlations of Asali and Hanratty (1985) and Henstock and Hanratty (1976). Asali correlated film thickness with liquid film Reynolds number in the ripple regime,

$$h_i^+ = 0.34\ Re_{LF}^{0.6} \qquad [30]$$

where

$$Re_{LF} = \frac{4\ \dot{m}_{LF}}{\pi\ D\ \mu_L} \qquad [31]$$

and $\dot{m}_{LF}$ is the liquid film mass flow rate. Henstock correlated film thickness with Re_{LF} in the disturbance wave regime,

$$h_i^+ = 0.0379\ Re_{LF}^{0.9}\ . \qquad [32]$$

When the film thickness is small relative to the tube diameter, Re_{LF} can be written

$$Re_{LF} = \frac{4\ h\ w_{avg}}{\nu_L}\ . \qquad [33]$$

Using [33] in [30] and solving for w_{avg}, a relation for the average liquid velocity in the ripple regime is found,

$$\frac{w_{avg}}{u_i^*} = 1.5\ h_i^{+\ 0.666}\ . \qquad [34]$$

Using [33] in [32] and solving for w_{avg}, a relation for the average liquid velocity in the disturbance wave regime is found,

$$\frac{w_{avg}}{u_i^*} = 9.5\ h_i^{+\ 0.111}\ . \qquad [35]$$

These relations can be combined into a single relation covering both regimes.

$$\frac{w_{avg}}{u_i^*} = \left[\left(1.5\ h_i^{+\ 0.666}\right)^{-2} + \left(9.5\ h_i^{+\ 0.111}\right)^{-2} \right]^{-0.5} \qquad [36]$$

Equation [36] has the limiting behaviors of [34] and [35]. At large h_i^+ the right hand side dominates, and at small h_i^+ the left hand side dominates. In the transition region between the two regimes both terms contribute to the predicted average velocity value.

Mass conservation

The fraction of the total liquid mass flow rate flowing as a film on the wall will be found by assuming the entrainment is known. The entrainment, E, is the ratio of the liquid mass flow rate suspended in the gas core, $\dot{m}_{LE}$, to the total liquid mass flow rate.

$$E = \dot{m}_{LE} / \dot{m}_L \qquad [37]$$

When the entrainment is known the liquid film mass flow rate can be calculated from

$$\dot{m}_{LF} = \dot{m}_L - \dot{m}_{LE}. \qquad [38]$$

The local film thickness and local average axial velocity are related to the mass flow rate in the liquid film by the integral

$$\dot{m}_{LF} = 2\, a\, \rho_L \int_0^{\pi} h\, w_{avg}\, d\bar{x}\,. \qquad [39]$$

Film thickness prediction

The set of simultaneous equations needed to solve for the film thickness distribution are summarized below.

Film thickness distribution

$$\frac{h^+}{h_o^+} = \frac{\ln\left[\alpha - \beta(\cos\bar{x} - 1)\right]}{\ln\alpha} \qquad [20]$$

where

$$\alpha = \exp\left(-\frac{h_o^+}{12}\right) \qquad [21]$$

$$\beta = \frac{1}{C_1\, Fr_{\tau_s}} \qquad [22]$$

$$h^+ = \frac{h}{\nu_L}\left(\frac{\tau_s}{\rho_L}\right)^{0.5} \qquad [14]$$

$$\tau_s = 0.023\ Re_{sg}^{-0.2} \rho_g\, u_g^2 \qquad [10]$$

and

$$Fr_{\tau_s} = \frac{\tau_s}{\rho_L\, g\, a} \qquad [23]$$

Theoretical prediction of the symmetry parameter

$$\frac{h_{avg}^+}{h_o^+} = \frac{\ln\left[\dfrac{\alpha + \beta + \sqrt{\alpha^2 + 2\,\alpha\,\beta}}{2}\right]}{\ln\alpha} \qquad [24]$$

Symmetry correlation curve fit (Equation [2] non-dimensionalized - valid only for $(\dot{m}_g / \dot{m}_L)^{0.5}\, Fr > 20$)

$$\frac{h_{avg}^+}{h_o^+} = 0.2 + 0.7\left[1 - \exp\left(-\frac{(\dot{m}_g / \dot{m}_L)^{0.5}\, Fr - 20}{75}\right)\right] \qquad [2]$$

where

$$Fr = U_{sg}/(gD)^{0.5} \qquad [3]$$

Interfacial axial shear correlation

$$\frac{\tau_i}{\tau_s} - 1 = 10\left(1 - \exp\left(-\frac{\phi\, h_i^+}{250}\right)\right) \qquad [29]$$

where

$$\phi = \frac{\mu_L}{\mu_g}\left(\frac{\rho_g}{\rho_L}\right)^{0.5} \qquad [26]$$

$$h_i^+ = \frac{h\, u_i^*}{\nu_L} \qquad [27]$$

and

$$u_i^* = \sqrt{\frac{\tau_i}{\rho_L}} \qquad [28]$$

Average liquid axial velocity

$$\frac{w_{avg}}{u_i^*} = \left[\left(1.5\, h_i^{+\,0.666}\right)^{-2} + \left(9.5\, h_i^{+\,0.111}\right)^{-2}\right]^{-0.5} \qquad [36]$$

Liquid film mass flow rate

$$\dot{m}_{LF} = 2\, a\, \rho_L \int_0^{\pi} h\, w_{avg}\, d\bar{x} \qquad [39]$$

$$E = \dot{m}_{LE} / \dot{m}_L \qquad [37]$$

and

$$\dot{m}_{LF} = \dot{m}_L - \dot{m}_{LE}\ . \qquad [38]$$

These equations can be solved at a given liquid and gas mass flow rate for a known experimental value of the entrainment. This was done for the film thickness distributions shown in figures 1 and 2 using the experimental entrainment values given in Laurinat (1982) at D = 5.08 cm. The predicted and experimental distributions are shown in figure 7a and 7b. The magnitude of C_1 for each curve is shown on the graphs.

Figure 8 shows model predictions compared to film thickness measurements taken by Dallman (1978) at D = 2.3 cm. Note the larger difference between the experimental value of h_{avg} / h_o and the h_{avg} / h_o value predicted from the symmetry correlation for the thicker of the two film distributions.

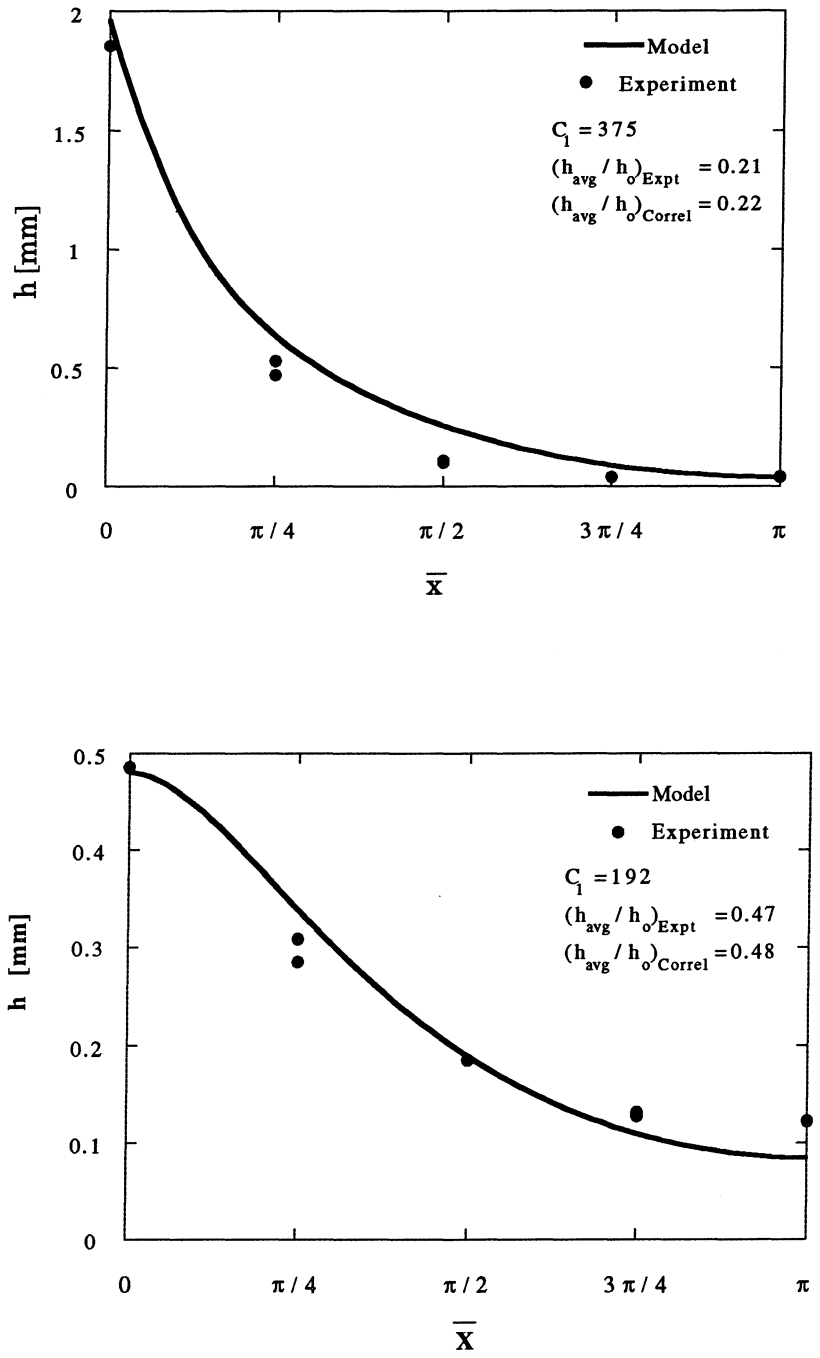

Figure 7a Model predictions compared to experimental data. Experimental air-water data from Laurinat (1982) in a 5.08 cm diameter horizontal tube at an L/D of 300. Flow conditions shown in figures 1 and 2.

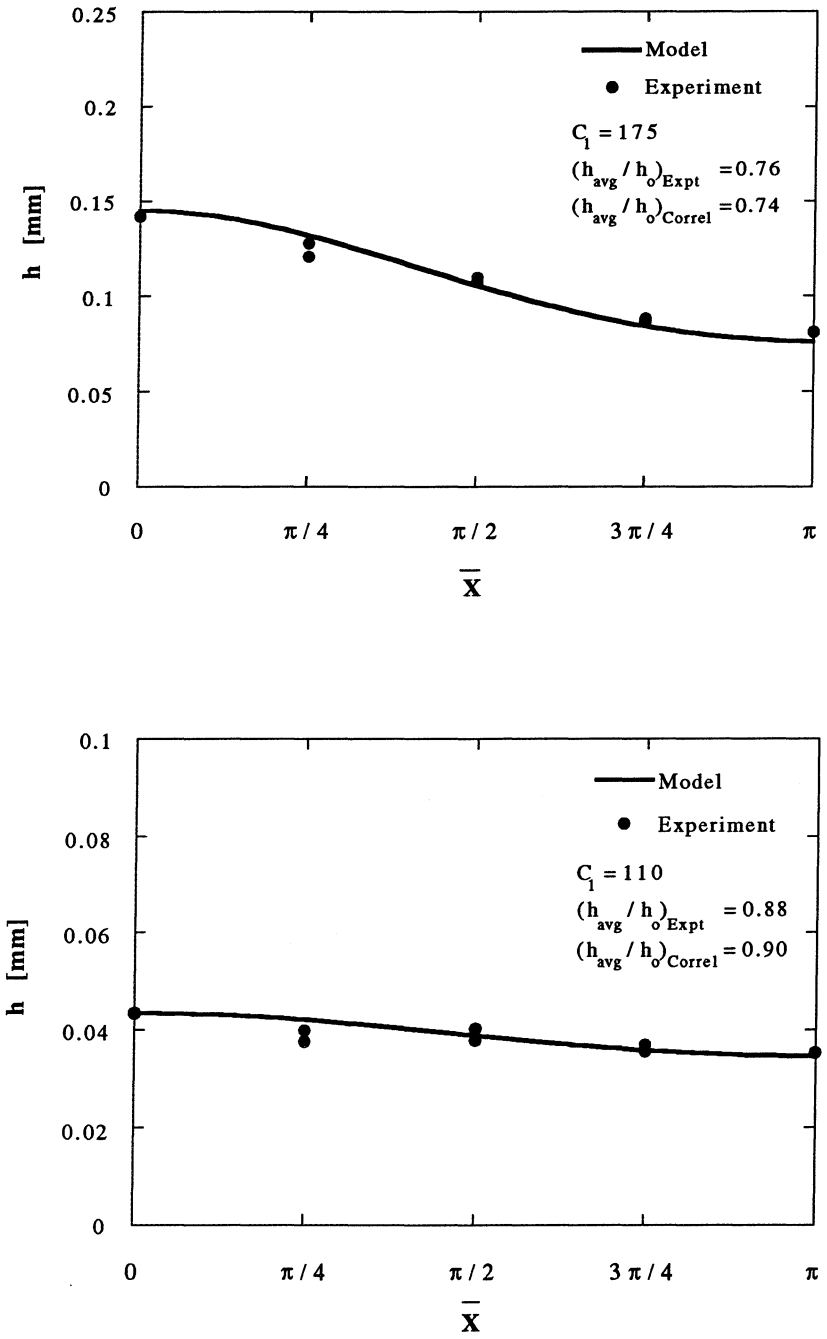

Figure 7b Model predictions compared to experimental data. Experimental air-water data from Laurinat (1982) in a 5.08 cm diameter horizontal tube at an L/D of 300. Flow conditions shown in figure 2.

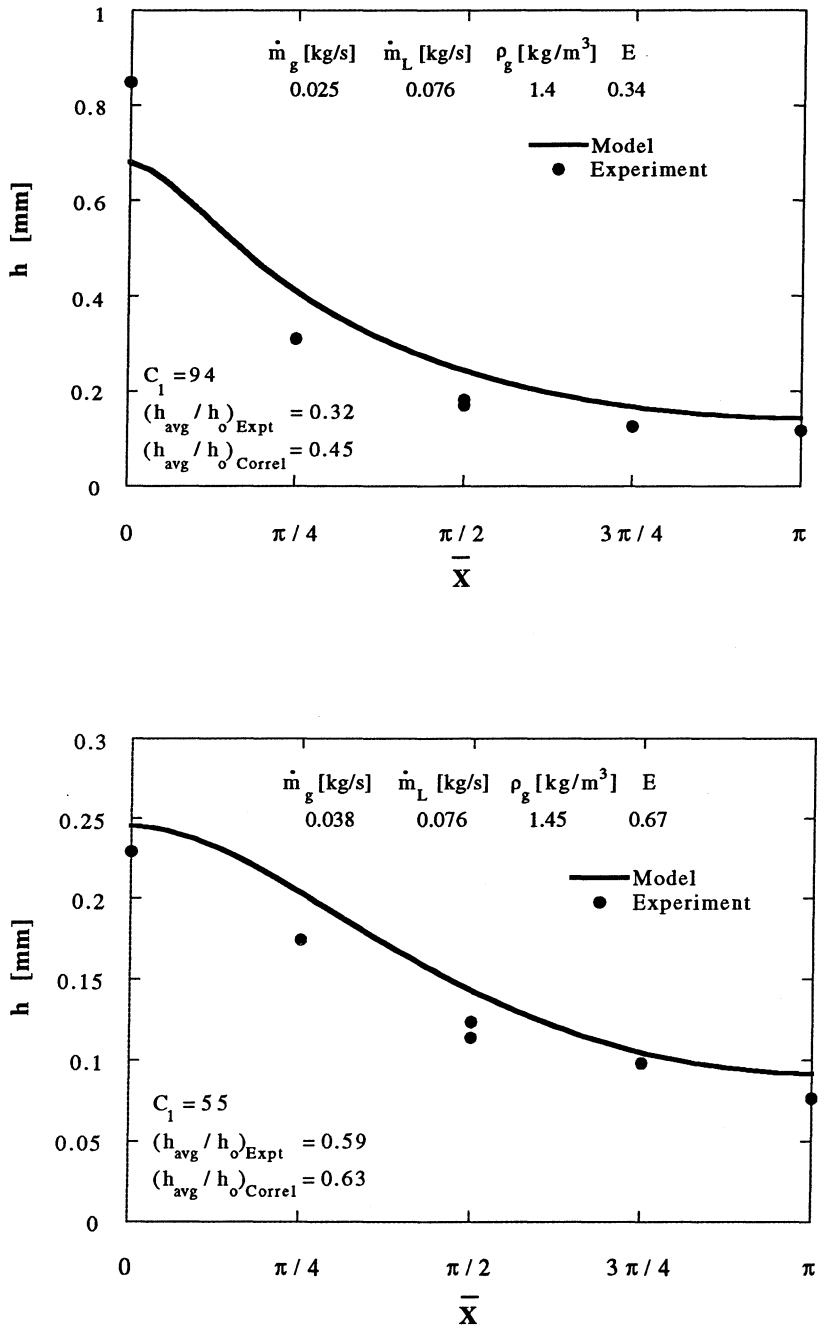

Figure 8 Model predictions compared to experimental data. Air-water data from Dallman (1978) in a 2.3 cm diameter horizontal tube at an L/D of 600.

3. DISCUSSION

The symmetry correlation builds on the work of Williams et al. (1996). It provides a method of predicting both qualitative and quantitative information about the flow regime.

Qualitatively, the symmetry correlation suggests a method for identifying flow regions based on the liquid and gas mass flow rates. The correlation shows a sharp rise in h_{avg} / h_o at the onset of asymmetric annular flow. This defines the boundary between the stratified-annular and asymmetric annular flow regions. A transition is seen where the flow becomes nearly symmetric. This defines the boundary between the asymmetric and symmetric annular regions.

Quantitatively, the symmetry correlation provides a prediction of the degree of circumferential symmetry. This is of value in film thickness modeling. It may also have value in the design of condensers and evaporators. Condensation conditions favor asymmetric films. Evaporators should operate in the symmetric film region as much as is practical. Operation in these regions can be more readily accomplished when the dependence of symmetry on gas and liquid mass flow rates is known.

The film thickness model is based on the work of Laurinat et al. (1985). Using the results of this study, a simplified model was developed. The value of this model is its simplicity, its range of applicability, and its method of determining the constant in the normal stress model. The model can be used to estimate the film thickness with reasonable accuracy over a wide range of annular flow conditions.

The predicted film thickness values do not show perfect agreement with the experimental data. This is to be expected due to the many simplifications of the model. The largest error occurs when the film is most asymmetrical in the stratified-annular flow region. The smallest error is found in the symmetric annular region.

The full model does not apply to films in which only part of the tube wall is wetted. At these conditions, the film thickness solution, [20], would likely predict negative values over a range of angles. The negative values would invalidate the theoretical estimate of the symmetry from equation [24] as well.

The sensitivity of the model to the symmetry correlation is seen in figure 8. The deviation of the model from the measured values is largely due to the model's poor estimate of the symmetry parameter for this condition. This is a weakness of the symmetry correlation in the rising asymmetric flow region where diameter may play a role in the onset of the steep rise.

Conditions may exist (due to tube diameter and/or mass flow rate) in which redistribution of the liquid film due to atomization and deposition and/or circumferential interfacial shear play a significant role in determining the average film thickness distribution. These conditions are not considered by the simplified model.

The model's circumferential normal stress is assumed to be a function of the local film thickness (equation [18]). The correlation for the axial interfacial shear is a function of the local film thickness as well (equation [25]). If stresses are caused primarily by the waves on the liquid surface, the film thickness dependence of the stress may be due to the film thickness dependence of the waves. Wave height has been observed to be proportional to film thickness. Hurlburt and Newell (1996) took instantaneous film thickness measurements in a 2.5 cm diameter tube and found the standard deviation of the film thickness to be proportional to and of similar order to the average film thickness.

The magnitude of the fluctuating velocities needed to balance the circumferential component of the weight of the liquid film can be calculated from the values of C_1. For the conditions considered in this paper the fluctuating velocities are at times as large as the liquid film's axial velocity. Experimental verification of the magnitude of the fluctuating velocities and thus the magnitude of the circumferential normal Reynolds stress gradient would help determine if the simplifications made to the momentum balance are in fact correct.

ACKNOWLEDGEMENTS

The authors appreciate the support of the Air Conditioning and Refrigeration Center at the University of Illinois at Urbana-Champaign under project 45. We also appreciate Professor Hanratty's sharing of his experience, insight, and enthusiasm.

REFERENCES

Asali, J. C., Hanratty, T. J., Andreussi, P. 1985 Interfacial drag and film height for vertical annular flow. AIChE J. **31**, 895-902.

Dallman, J. C. 1978 Investigation of separated flow model in annular-gas liquid two-phase flows. Ph.D. thesis, University of Illinois, Urbana.

Fukano, T., Ousaka, A. 1989 Prediction of the circumferential distribution of film thickness in horizontal and near-horizontal gas-liquid annular flows. Int. J. Multiphase Flow **15**, 403-419.

Henstock, W. H., Hanratty, T. J. 1976 The interfacial drag and the height of the wall layer in annular flows. AIChE J. **22**, 990-1000.

Hewitt, G. F., Jayanti, S., Hope, C. B. 1990 Structure of thin liquid films in gas-liquid horizontal flow. Int. J. Multiphase Flow **16**, 951-957.

Hurlburt, E. T., Newell, T. A. 1996 Optical measurement of liquid film thickness and wave velocity in liquid film flows. Experiments in Fluids **21**, 357-362.

Jayanti, S., Hewitt, G. F., White, S. P. 1990 Time-dependent behaviour of the liquid film in horizontal annular flow. Int. J. Multiphase Flow **16**, 1097-1116.

Laurinat, J. E. 1982 Studies of the effect of pipe size on horizontal annular two-phase flows. Ph.D. thesis, University of Illinois, Urbana.

Laurinat, J. E., Hanratty, T. J., Jepson, W. P. 1985 Film thickness distribution for gas-liquid annular flow in a horizontal pipe. PhysicoChem. Hydrodynam. **6**, 179-195.

Lin, T. F., Jones, O. C., Lahey, R. T., Block, R. C., Murase, M. 1985 Film thickness measurements and modelling in horizontal annular flows. PhysicoChem. Hydrodynam. **6**, 197-206.

Paras, S. V., Karabelas, A. J. 1991 Properties of the liquid layer in horizontal annular flow. Int. J. Multiphase Flow **17**, 439-454.

Sutharshan, B., Kawaji, M., Ousaka, A. 1995 Measurement of circumferential and axial liquid film velocities in horizontal annular flow. Int. J. Multiphase Flow **21**, 193-206.

Whalley, P. B. 1987 Boiling, Condensation, and Gas-Liquid Flow. Clarendon Press, Oxford.

Williams, L. R. 1990 Effect of pipe diameter on horizontal annular two-phase flow. Ph.D. thesis, University of Illinois, Urbana.

Williams, L. R., Dykhno, L. A., Hanratty, T. J. 1996 Droplet flux distributions and entrainment in horizontal gas-liquid flows. Int. J. Multiphase Flow **22**, 1-18.